The Control of Airplane Landing in Longitudinal and Lateral-directional Planes by using the H-inf Control

Mihai Lungu, Romulus Lungu
University of Craiova, Faculty of Electrical Engineering, Craiova, Romania
Lma1312@yahoo.com, romulus_lungu@yahoo.com

***Abstract*—This work presents the automatic control of airplane in longitudinal and lateral-directional planes, during landing, by using the H-inf control and the airplane's linearized dynamics; the H-inf control technique assures robust stability with respect to different disturbances and noise type signals. Both the longitudinal plane and the lateral-directional one are treated; three automatic landing subsystems (ALSs) are obtained: the first two control airplane's motion in longitudinal plane, while the third one is employed for the airplane's control in lateral-directional plane. Before the landing's two main stages in longitudinal plane, the pilot must cancel the airplane's lateral deviation with respect to the runway in lateral plane. The three subsystems have been designed separately and put together to form a single ALS. The complete ALS has been software implemented, tested, and validated through numerical simulations; promising results have been obtained.**

Keywords— landing; airplane; H-inf control

I. INTRODUCTION

Landing is a difficult flight stage; airplanes have to perform precise maneuvers near the ground to land in safely conditions, at desired touch points with satisfactory sink rate, attitude, and speed [1]. There are many methods to design automatic landing systems; for airplane's control in lateral-directional plane, in [2] and [3] there has been designed an Instrumental Landing System based ALS; it contains a radio-navigation system and a system for obtaining the distances between the airplane and the runway radio-markers. Such ALSs have PD/PI/PID controllers, classical or fuzzy ones [4] etc. In the optimal synthesis research area, Ochi & Kanai used the H-inf control approach to design controllers for airplanes' automatic landing [5], but their robustness has been not analyzed with respect to sensor errors and wind shears; this is completed in work [6], where for linear and nonlinear airplane's dynamics, PD fuzzy control ALS is designed and validated; moreover, in [7], the ALS's robustness with respect to different initial conditions is proved. The presence of known nonlinearities associated to the dynamics of airplane or actuators as well as to the external disturbances motivates the need of adaptive control architectures consisting of neural networks and Pseudo Control Hedging blocks [8, 9]. Other automatic landing system (ALS) has been designed in [10] using a back-propagation learning algorithm based feed-forward neural networks; the main disadvantage is that the neural networks require a priori training on normal and faulty operating data. Other approaches involving time delay NNs [11] are characterized by insufficient flight path's track accuracy and limited operating conditions. The main disadvantages of the NN based approaches designed in [11, 12] are the required operating conditions (difficult to be satisfied in practical control applications). Also, the main weakness of the papers dealing with landing is that the automatic landing systems have been designed for the longitudinal plane or for the lateral-directional one. The present paper focuses on airplane's automatic control in the two planes using the H-inf control. Our purpose is to design and validate a new ALS (both planes) cancelling the negative effect of possible disturbances (errors of the sensors, crosswind, or wind shears).

The paper's organization includes: 1) the dynamics of the airplane in the two planes as well as its control during the landing's main two stages in longitudinal plane; 2) the design of the subsystem for the control of airplane in lateral-directional plane (third section of the paper); 3) the validation of the new designed ALS by means of complex simulations and a brief analysis of the obtained results; 4) remarks and conclusions regarding the new designed ALS (fifth section of the paper).

II. AIRPLANE'S CONTROL IN LONGITUDINAL PLANE

A. Airplane dynamics in the two planes

The procedure of landing includes three main phases: initial approach, glide slope, and flare [13]. The initial approach is equivalent with the airplane's descent from the cruise altitude to an altitude of 420 m for heavy airplane or less (light airplane). The next step is the positioning of airplane such that it is on a heading towards the runway centerline [14]. During next two stages, both in longitudinal plane, the speed and the altitude must be controlled; at to 7-20 m above the ground, the system for the control of slope angle is no more useful and the flare maneuver begins [15]. In order to have a soft impact with the surface of the runway and the landing gear to dissipate all the impact energy, one has to decrease the vertical descent rate. After that, the airplane's pitch angle is modified (between 0 and 5 deg.) for a soft contact with the runway [16]. These targets will be achieved using the first two control systems to be designed in this paper (automatic landing systems for the control of airplane's trajectory in longitudinal plane). On the other hand, there must be also canceled, by means of flight direction automatic control systems, the positioning errors in the lateral plane, the most important error being airplane's lateral deviation with respect to the runway; for this aim, there will be designed another control system (the third one) for the control of airplane's trajectory in lateral-directional plane. In Fig. 1, there are presented the main elements of airplane's geometry relative to runway – longitudinal and lateral-directional planes; in Fig. 1, PA is the glide slope, PDA – the runway, γ_c – the trajectory's desired slope angle, R – the distance between the

978-1-5090-4862-5/17/$31.00 ©2017 IEEE

radio-marker and the airplane, γ – the slope angle, Y – the lateral deviation of the airplane relative to the runway, $\overline{\psi}$ – the runway's direction, ψ – the flight direction, β – the glide slope angle. The expression of the angle Γ is [17]:

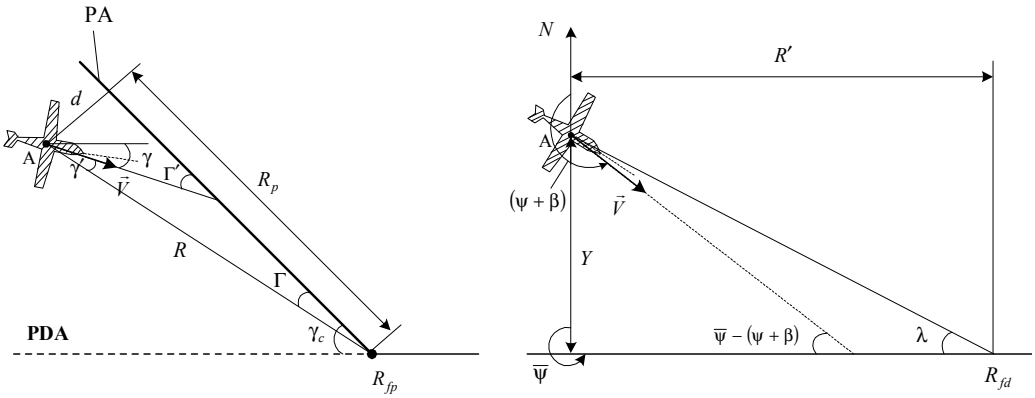

a. b.

Fig. 1. The geomtery of motions: a) longitudinal plane; b) lateral-directional plane

$$\Gamma = \frac{1}{R}\int_0^t V\Gamma' d\tau = \frac{1}{R}\int_0^t V(\gamma_c - \gamma)d\tau \cong \frac{V_0}{R}\int_0^t V(\gamma_c - \gamma)d\tau. \quad (1)$$

The linearized dynamics used in this paper for airplane's motion in longitudinal plane belongs to a Boeing 747 [17]:

$$\begin{aligned} \dot{x} &= Ax + Bu, \\ y_e &= Cx, \end{aligned} \quad (2)$$

with $\boldsymbol{x} \in R^{5\times 1}$ – the state vector, $x = \begin{bmatrix} V_x & V_z & \omega_y & \theta & \delta_T \end{bmatrix}^{\mathrm{T}}$, and $u = \delta_{T_c}$ – the control input; V_x and V_z are the airplane speed components along its longitudinal and normal axes, ω_y – the pitch angular rate, θ – the pitch angle, while δ_T is the engine's command. The state variable δ_T verifies the equation: $T\dot{\delta}_T + \delta_T = \delta_{T_c}$; T – engine time constant. The matrices A, B, and C are respectively [17]:

$$A = \begin{bmatrix} a_{11} & a_{12} & a_{13} & a_{14} & b_{12} \\ a_{21} & a_{22} & a_{23} & a_{24} & b_{22} \\ a_{31} & a_{32} & a_{33} & a_{34} & b_{32} \\ 0 & 0 & 1 & 0 & 0 \\ 0 & 0 & 0 & 0 & -\frac{1}{T} \end{bmatrix}, B = \begin{bmatrix} 0 \\ 0 \\ 0 \\ 0 \\ \frac{1}{T} \end{bmatrix}, C^{\mathrm{T}} = \begin{bmatrix} 1 & 0 \\ 0 & -\frac{1}{V_0} \\ 0 & 0 \\ 0 & 1 \\ 0 & 0 \end{bmatrix}; \quad (3)$$

the output vector has been chosen as: $y_e = \begin{bmatrix} V_x & \gamma \end{bmatrix}^{\mathrm{T}}; \gamma = \theta - \alpha = \theta - \frac{1}{V_0}V_z$, where $V_0 \cong V_{x_0}$ is the nominal value of the airplane's forward velocity.

B. Airplane control during glide slope

To control the longitudinal velocity V_x and the slope angle γ (thus, to control the angle Γ), one introduces the state vector: $x_c = \begin{bmatrix} x_{c_1} & x_{c_2} & x_{c_3} \end{bmatrix}^{\mathrm{T}} = \left[\frac{1}{T\mathrm{s}+1}(\overline{V}_x - V_x) \quad \frac{V_0}{\mathrm{s}}(\gamma_c - \gamma) \quad \frac{1}{\mathrm{s}}(\overline{\Gamma} - \Gamma) \right]^{\mathrm{T}}$, where $\overline{V}_x, \gamma_c, \overline{\Gamma}$ are the imposed values of the variables V_x, γ, Γ. According to the last equation, the supplementary vector x_c depends on the system's state vector x, i.e. [18]: $\dot{x}_c = A_{21}x + A_{22}x_c + B_{21}u_c + B_{22}u$, with $u_c = \begin{bmatrix} \overline{V}_x & \gamma_c & \overline{\Gamma} \end{bmatrix}^{\mathrm{T}}$. Taking into account the expression of y_e and the last form of (1), one obtains: $\dot{x}_{c_1} = \frac{1}{T}\left(-V_x - x_{c_1} + \overline{V}_x\right), \dot{x}_{c_2} = -V_0\theta + V_z + V_0\gamma_c, \dot{x}_{c_3} = \overline{\Gamma} - \frac{1}{R_0}x_{c_2}$. From these equations and expression of $\dot{x}_c$, it results:

$$A_{21} = \begin{bmatrix} -\frac{1}{T} & 0 & 0 & 0 & 0 \\ 0 & 1 & 0 & -V_0 & 0 \\ 0 & 0 & 0 & 0 & 0 \end{bmatrix}, A_{22} = \begin{bmatrix} -\frac{1}{T} & 0 & 0 \\ 0 & 0 & 0 \\ 0 & -\frac{1}{R_0} & 0 \end{bmatrix}, B_{21} = \begin{bmatrix} \frac{1}{T} & 0 & 0 \\ 0 & V_0 & 0 \\ 0 & 0 & 1 \end{bmatrix}, B_{22} = \begin{bmatrix} 0 \\ 0 \\ 0 \end{bmatrix}.$$

One chooses the output vector $z = \begin{bmatrix} z_1 & z_2 & z_3 \end{bmatrix}^{\mathrm{T}} = \begin{bmatrix} c_1 x_{c_1} & c_2 x_{c_3} & c_3 \delta_{T_c} \end{bmatrix}^{\mathrm{T}}$, where c_1, c_2, c_3 are positive constants; the vector z can be written under the form:

$$z = C_{11}x + C_{12}x_c + D_{11}u_c + D_{12}u. \quad (4)$$

By identification, there are obtained: $C_{11} = 0_{3\times 5}, D_{11} = 0_{3\times 3}$, $C_{12} = \begin{bmatrix} c_1 & 0 & 0 \\ 0 & 0 & c_2 \\ 0 & 0 & 0 \end{bmatrix}, D_{12} = \begin{bmatrix} 0 \\ 0 \\ c_3 \end{bmatrix}$. The output vector used for achieving the airplane control in glide slope phase is expressed as:

$$\begin{aligned} &y = C_{21}x + C_{22}x_c + D_{21}u_c + D_{22}u, \\ &C_{21} = \begin{bmatrix} I_{5\times 5} \\ 0_{3\times 5} \end{bmatrix}, C_{22} = \begin{bmatrix} 0_{5\times 3} \\ I_{3\times 3} \end{bmatrix}, \\ &D_{21} = 0_{8\times 3}, D_{22} = 0_{8\times 1}. \end{aligned} \quad (5)$$

Moreover, the first equation (2) can be put under the form: $\dot{x} = A_{11}x + A_{12}x_c + B_{11}u_c + B_{12}u$, with $A_{11} = A, A_{12} = 0_{5\times 3}, B_{11} = 0_{5\times 3}$, $B_{12} = B$; putting together the expressions of $\dot{x}, \dot{x}_c, z$, and y, one obtains the following equation:

$$\begin{bmatrix}\dot{x}\\ \dot{x}_c\\ z\\ y\end{bmatrix}=\left[\begin{array}{cc|c:c}A_{11} & A_{12} & B_{11} & B_{12}\\ A_{21} & A_{22} & B_{21} & B_{22}\\ \hline C_{11} & C_{12} & D_{11} & D_{12}\\ \cdots & \cdots & \cdots & \cdots\\ C_{21} & C_{22} & D_{21} & D_{22}\end{array}\right]\begin{bmatrix}x\\ x_c\\ u_c\\ u\end{bmatrix}=\left[\begin{array}{c|c:c}\overline{A} & B_1 & B_2\\ \hline \overline{C}_1 & D_{11} & D_{12}\\ \cdots & \cdots & \cdots\\ C_2 & D_{21} & D_{22}\end{array}\right]\begin{bmatrix}x\\ x_c\\ u_c\\ u\end{bmatrix}. \quad (6)$$

The control law is chosen of the following form: $u=-Ky=$ $=-\begin{bmatrix}K_1 & K_2\end{bmatrix}\begin{bmatrix}x^{\mathrm{T}} & x_c^{\mathrm{T}}\end{bmatrix}^{\mathrm{T}}, K=B_2^{\mathrm{T}}P_\infty$, with $P_\infty\in R^{8\times 8}$ – the solution of the Riccati matrix equation [17]:

$$\overline{A}^{\mathrm{T}}P_\infty+P_\infty\overline{A}+P_\infty\left[\mu^{-2}B_1B_1^{\mathrm{T}}-B_2\left(D_{12}^{\mathrm{T}}D_{12}\right)^{-1}B_2^{\mathrm{T}}\right]P_\infty+C_1^{\mathrm{T}}C_1=0, \quad (7)$$

where μ is a constant that must be minimized, $C_1=\begin{bmatrix}C_{11} & C_{12}\end{bmatrix}$, $B_1=\begin{bmatrix}B_{11}^{\mathrm{T}} & B_{21}^{\mathrm{T}}\end{bmatrix}^{\mathrm{T}}, B_2=\begin{bmatrix}B_{12}^{\mathrm{T}} & B_{22}^{\mathrm{T}}\end{bmatrix}^{\mathrm{T}}$. The block diagram of this first subsystem for the control of landing (glide slope phase) is given in Fig. 2.

C. *Airplane control during flare*

In this case, in the state vector x, the altitude H is introduced; the equation associated to this new state is: $\dot{H}=-\frac{1}{\tau}H$. Thus, the new state vector becomes: $x=\begin{bmatrix}V_x & V_z & \omega_y & \theta & H & \delta_T\end{bmatrix}^{\mathrm{T}}$, while the matrices (3) get the forms:

$$A=\begin{bmatrix}a_{11} & a_{12} & a_{13} & a_{14} & 0 & b_{12}\\ a_{21} & a_{22} & a_{23} & a_{24} & 0 & b_{22}\\ a_{31} & a_{32} & a_{33} & a_{34} & 0 & b_{32}\\ 0 & 0 & 1 & 0 & 0 & 0\\ 0 & 0 & 0 & 0 & -\frac{1}{\tau} & 0\\ 0 & 0 & 0 & 0 & 0 & -\frac{1}{T}\end{bmatrix}, B=\begin{bmatrix}0\\ 0\\ 0\\ 0\\ 0\\ \frac{1}{T}\end{bmatrix}, C=\begin{bmatrix}1&0&0&0&0&0\\ 0&1&0&0&0&0\\ 0&0&0&1&0&0\\ 0&0&0&0&1&0\end{bmatrix}; \quad (8)$$

one has chosen as output vector – $y_e=\begin{bmatrix}V_x & V_z & \theta & H\end{bmatrix}^{\mathrm{T}}$. Now, the variable x_{c_2} has other form, while x_{c_1} is the same. The expression of $\dot{H}$ can be written as [17]: $\dot{H}=V_{x_0}\theta-V_z$; between the two equations of $\dot{H}$ there is a difference (error): $e_{\dot{h}}=\dot{H}+\frac{1}{\tau}H$, that must tend to an imposed value $\bar{e}_{\dot{h}}=0$. In order to have $e_{\dot{h}}=\bar{e}_{\dot{h}}$, after the deviation $\tilde{e}_{\dot{h}}=\bar{e}_{\dot{h}}-e_{\dot{h}}$ one will introduce an ideal integrator on the subsystem direct way; thus, it appears another state: $x_{c_2}=\frac{1}{\mathrm{s}}\tilde{e}_{\dot{h}}$. Therefore, $x_c=\begin{bmatrix}x_{c_1} & x_{c_2}\end{bmatrix}^{\mathrm{T}}$ and $u_c=\begin{bmatrix}\overline{V}_x & \bar{e}_{\dot{h}}\end{bmatrix}^{\mathrm{T}}$. As in the first case (glide slope), one gets:

$$\dot{x}_{c_1}=\frac{1}{T}\left(-V_x-x_{c_1}+\overline{V}_x\right), \dot{x}_{c_2}=\bar{e}_{\dot{h}}-e_{\dot{h}}\Leftrightarrow\dot{x}_{c_2}=-\frac{1}{\tau}H-\dot{H}+\bar{e}_{\dot{h}}\Leftrightarrow$$

$$\Leftrightarrow\dot{x}_{c_2}=-V_{x_0}\theta+V_z-\frac{H}{\tau}+\bar{e}_{\dot{h}}; A_{21}=\begin{bmatrix}-\frac{1}{T} & 0 & 0 & 0 & 0 & 0\\ 0 & 1 & 0 & -V_0 & -\frac{1}{\tau} & 0\end{bmatrix},$$

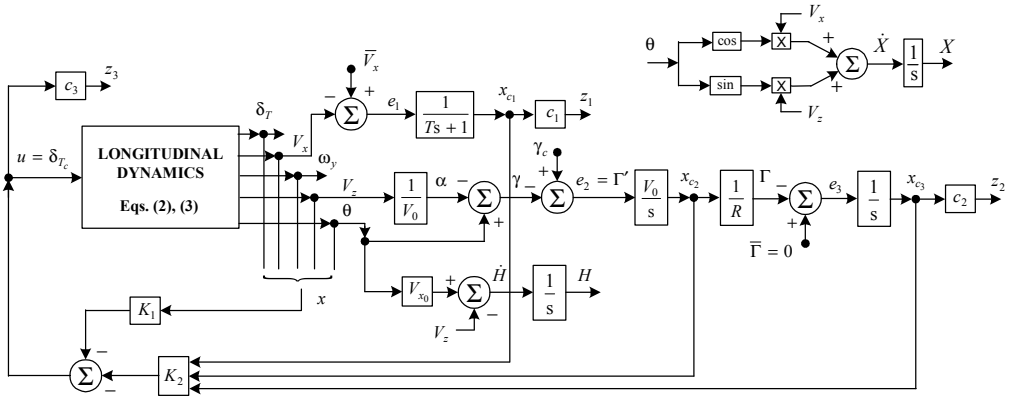

Fig. 2. Airplane control subsystem during glide slope phase (longitudinal plane)

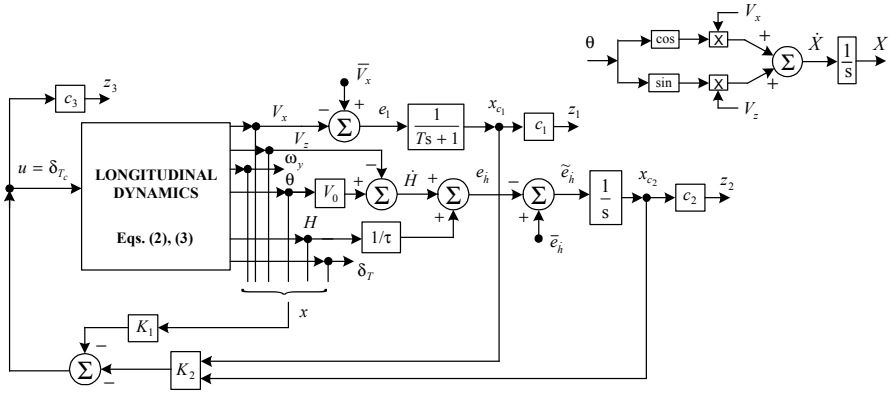

Fig. 3. Airplane control subsystem during flare phase (longitudinal plane)

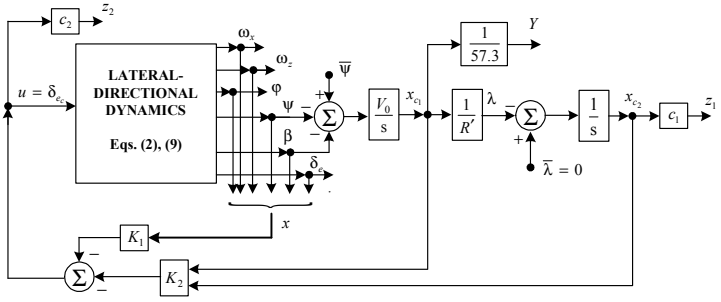

Fig. 4. Airplane control subsystem during initial approach (lateral-directional plane)

$$A_{22}=\begin{bmatrix}-\frac{1}{T} & 0\\ 0 & 0\end{bmatrix}, B_{21}=\begin{bmatrix}\frac{1}{T} & 0\\ 0 & 1\end{bmatrix}, B_{22}=0_{2\times 1}.$$

One chooses the output vector:

$$\begin{aligned} &z=\left[z_1\ \ z_2\ \ z_3\right]^{\mathrm{T}}=\left[c_1x_{c_1}\ \ c_2x_{c_2}\ \ c_3\delta_{T_c}\right]^{\mathrm{T}},\\ &z=C_{11}x+C_{12}x_c+D_{11}u_c+D_{12}u, \end{aligned} \tag{9}$$

with $C_{11}=0_{3\times 6}, D_{11}=0_{3\times 2}, C_{12}=\begin{bmatrix}c_1 & 0\\ 0 & c_2\\ 0 & 0\end{bmatrix}, D_{12}=\begin{bmatrix}0\\ 0\\ c_3\end{bmatrix}$. The output vector y is: $y=\left[x^{\mathrm{T}}\ \ x_c^{\mathrm{T}}\right]^{\mathrm{T}}=\left[V_x\ V_z\ \omega_y\ \theta\ H\ \delta_T\ x_{c_1}\ \ x_{c_2}\right]^{\mathrm{T}}$, which can be put under the form (5) with $C_{21}=\begin{bmatrix}I_{6\times 6}\\ 0_{2\times 6}\end{bmatrix}, C_{22}=\begin{bmatrix}0_{6\times 2}\\ I_{2\times 2}\end{bmatrix}$, $D_{21}=0_{8\times 2}, D_{22}=0_{8\times 1}$; also, in this case, $A_{11}=A, A_{12}=0_{6\times 2}$, $B_{11}=0_{6\times 2}, B_{12}=B$. The control law is calculated as in the first case. The block diagram of the second subsystem for the control of landing (flare phase) is presented in Fig. 3.

III. Airplane's Control in Lateral-Directional Plane

The third main subsystem of the new designed ALS must cancel airplane's lateral deviation with respect to the runway [1]; only one command (aileron command) will be used.

The state vector and the command of the system are: $x=\left[\beta\ \omega_x\ \omega_z\ \varphi\ \psi\ \delta_e\right]^{\mathrm{T}}, u=\delta_{e_c}$, where δ_e (aileron command) verifies the equation: $\dot{\delta}_e=-\frac{1}{T_e}\delta_e+\frac{1}{T_e}\delta_{e_c}$ (T_e – time constant); φ and ψ are the roll and yaw angles, while ω_x and ω_z are the roll and yaw angular rates, respectively. With these, the matrices A and B from airplane dynamics are, respectively:

$$A=\begin{bmatrix}a_{11} & a_{12} & a_{13} & a_{14} & 0 & b_{11}\\ a_{21} & a_{22} & a_{23} & 0 & 0 & b_{21}\\ a_{31} & a_{32} & a_{33} & 0 & 0 & b_{31}\\ 0 & 1 & 0 & 0 & 0 & 0\\ 0 & 0 & 1 & 0 & 0 & 0\\ 0 & 0 & 0 & 0 & 0 & -\frac{1}{T_e}\end{bmatrix}, B=\begin{bmatrix}0\\ 0\\ 0\\ 0\\ 0\\ \frac{1}{T_e}\end{bmatrix}. \tag{10}$$

The supplementary state vector is chosen of the form [17]:

$$x_c=\left[x_{c_1}\ \ x_{c_2}\right]^{\mathrm{T}}=\left[\frac{V_0}{\mathrm{s}}\left(\bar{\psi}-\psi-\beta\right)\ \ \frac{1}{\mathrm{s}}\left(\bar{\lambda}-\lambda\right)\right]^{\mathrm{T}}, \tag{11}$$

such that, in stationary regime, one gets: $\psi+\beta=\bar{\psi}$ and $\lambda=\bar{\lambda}=0$. The derivatives of the vector x_c satisfy the equations: $\dot{x}_{c_1}=-V_0\beta-V_0\psi+V_0\bar{\psi}, \dot{x}_{c_2}=-\frac{1}{R'}x_{c_1}+\bar{\lambda}, u_c=\left[\bar{\psi}\ \ \bar{\lambda}\right]^{\mathrm{T}}$; the next matrices are obtained: $A_{21}=\begin{bmatrix}-V_0 & 0 & 0 & 0 & -V_0 & 0\\ 0 & 0 & 0 & 0 & 0 & 0\end{bmatrix}, A_{22}=\begin{bmatrix}0 & 0\\ -\frac{1}{R'} & 0\end{bmatrix}$, $B_{21}=\begin{bmatrix}V_0 & 0\\ 0 & 1\end{bmatrix}, B_{22}=\begin{bmatrix}0\\ 0\end{bmatrix}$. The form of the output vector is $z=\left[z_1\ \ z_2\right]^{\mathrm{T}}=\left[c_1x_{c_2}\ \ c_2\delta_{e_c}\right]^{\mathrm{T}}$; z verifies (4) with $C_1=0_{2\times 6}$, $D_{11}=0_{2\times 2}, C_{12}=\begin{bmatrix}0 & c_1\\ 0 & 0\end{bmatrix}, D_{12}=\begin{bmatrix}0\\ c_2\end{bmatrix}$. The vector necessary for the control is $y=\left[x^{\mathrm{T}}\ \ x_c^{\mathrm{T}}\right]^{\mathrm{T}}=\left[\beta\ \omega_x\ \omega_z\ \varphi\ \psi\ \delta_e\ x_{c_1}\ \ x_{c_2}\right]^{\mathrm{T}}$; it verifies the first equation (5) with $C_{21}=\begin{bmatrix}I_{6\times 6}\\ 0_{2\times 6}\end{bmatrix}, C_{22}=\begin{bmatrix}0_{6\times 2}\\ I_{2\times 2}\end{bmatrix}$, $D_{21}=0_{8\times 2}, D_{22}=0_{8\times 1}$. Using these, the matrix from (6) is formed; it is used to the obtaining of the matrix K as function of $P_\infty\in R^{8\times 8}$ – solution of the Riccati equation (7). The block diagram of the subsystem for the airplane's control in lateral-directional plane is given in Fig. 4.

IV. Numerical Simulation Results

To study the performances of the new obtained automatic landing system (having three subsystems – two for the control in longitudinal plane (Figs. 2 and 3) and one for the control in lateral-directional plane – Fig. 4), we consider the landing of a Boeing 747 airplane. Complex simulations in Matlab/Simulink environment have been performed. For the longitudinal plane, the values of the coefficients from the block diagram in Fig. 2 are [17, 19]: $V_0=67\,\mathrm{m/s}, c_1=50, c_2=30, c_3=10, \mu=5.1\cdot 10^{-4}$, $\left[\bar{V}_x\ \ \gamma_c\ \ \bar{\Gamma}\right]^{\mathrm{T}}=\left[V_0\ \ -2.5^\circ\ \ 0\right]^{\mathrm{T}}, H_p=H(0)=60\,\mathrm{m}, x_p=x(0)=0$, $R_0=1800\,\mathrm{m}, x_{c_1}(0)=0\,\mathrm{m}, x_{c_2}(0)=0\,\mathrm{m}, x_{c_3}(0)=3\,\mathrm{m}, x_0=$ $=\left[70\,\mathrm{m/s}\ \ 2\,\mathrm{m/s}\ \ 1\,\mathrm{grd/s}\ \ 2\,\mathrm{grd}\ \ 0\right]^{\mathrm{T}}$; for flare (the subsystem in Fig. 3), one used the values [17, 19]: $T=0.01\mathrm{s}, \tau=6\mathrm{s}, H_0=$ $=20\mathrm{m}, c_1=5, c_2=2, c_3=1, \left[\bar{V}_x\ \ \bar{e}_h\right]^{\mathrm{T}}=\left[67\mathrm{m/s}\ \ 0\mathrm{m/s}\right]^T, \mu=0.107$, $R'=6000$ m. The coefficients of matrix A are: $a_{11}=-0.021$,

$a_{12}=0.122, a_{13}=0, a_{14}=-9.69, a_{21}=-0.201, a_{22}=-0.7535,$
$a_{23}=67, a_{24}=0, a_{31}=0, a_{32}=-0.24569, a_{33}=-0.2136, a_{34}=0,$
$b_{12}=0.1, b_{22}=b_{32}=0$. In Figs. 5 and 6 one represents the time characteristics for the two landing phases in longitudinal plane. At H=H_0=20 m (altitude for starting of the glide slope), there will be considered the time origin for the flare phase. One may remark in Figs. 5 and 6 that slope angle is in accordance with its theoretical values: -2.5 deg for the glide slope and 0 deg for the flare. During glide slope, airplane follows a descending trajectory (8th graphic in Fig. 5.), while the flare trajectory is parabolic (8th graphic in Fig. 6) with null slope angle.

For lateral-directional plane, the coefficients from Fig. 4 are [17, 19]: $V_0=67\text{m/s}, T_e=0.1\text{s}, c_1=5, c_2=2, \mu=7, [\overline{\psi}\ \overline{\lambda}]^{\text{T}}=[0\ 0]^{\text{T}}$, $R_0'=6700\,\text{m}, x(0)=[0.5\,\text{grd}\ \ 2\,\text{grd/s}\ \ 1\,\text{grd/s}\ \ 2\,\text{grd}\ \ 1\,\text{grd}\ \ 5\,\text{grd}]^{\text{T}}$, $x_c(0)=[0\ \ 0]^{\text{T}}$. The coefficients of matrix A are: $a_{11}=-0.001$, $a_{12}=0, a_{13}=-1, a_{14}=0.15, a_{21}=-1.33, a_{22}=-0.98, a_{23}=0.33, a_{31}=0.17,$
$a_{32}=-0.17, a_{33}=-0.217, a_{33}=0.2136, b_{11}=0, b_{21}=0.23, b_{31}=0.026.$
The time characteristics associated to initial approach phase (lateral-directional plane) are presented in Fig. 7; one remarks that the subsystem responds very well and the cancelling of the airplane's lateral deviation relative to the runway $(Y\to 0)$.

The problem of landing based on the design of new ALSs has also been discussed in other papers such as [7, 19-21]. If a brief comparison between our ALS (having three subsystems– Figs. 2, 3, and 4) and the Instrumental Landing System based ALS or conventional/fuzzy controllers based ALSs [19] is achieved, one may remark that the ALS based on H-inf technique is slightly better from the point of view of the transient regime period and overshoot. The performances' improvement was obtained using fuzzy controllers instead of conventional ones[21], but the obtained ALSs are ineffective in the case of

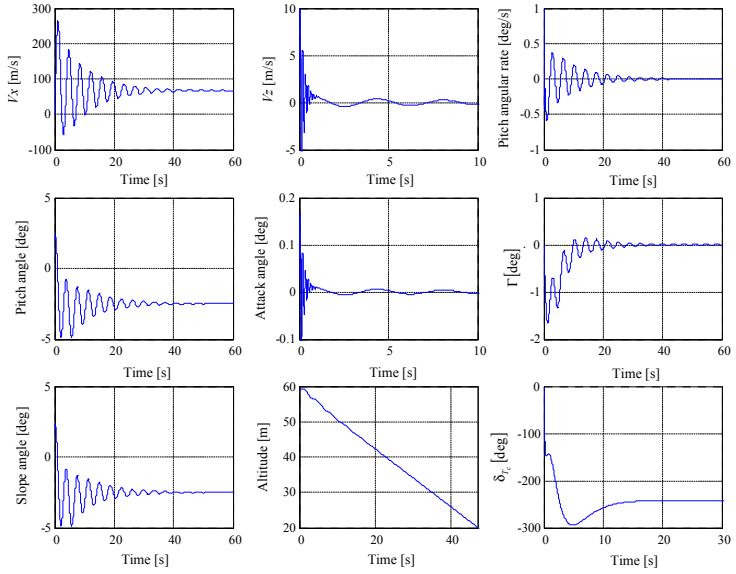

Fig. 5. Time characteristics associated to the glide slope phase

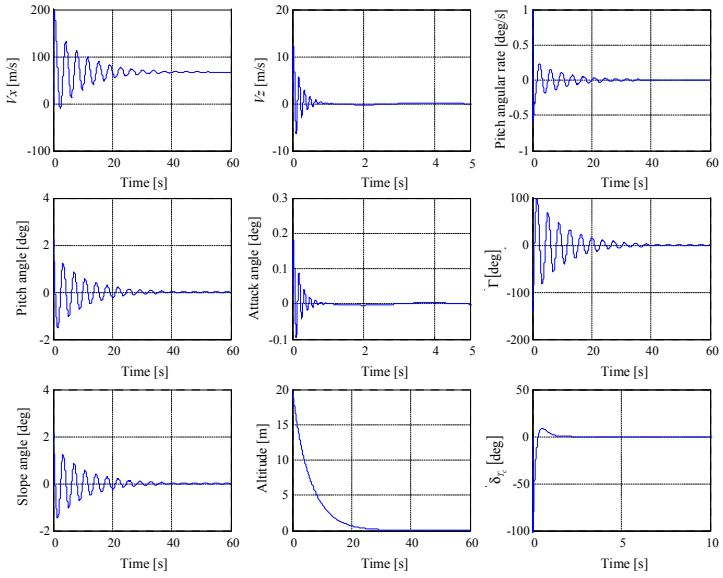

Fig. 6. Time characteristics associated to the flare phase

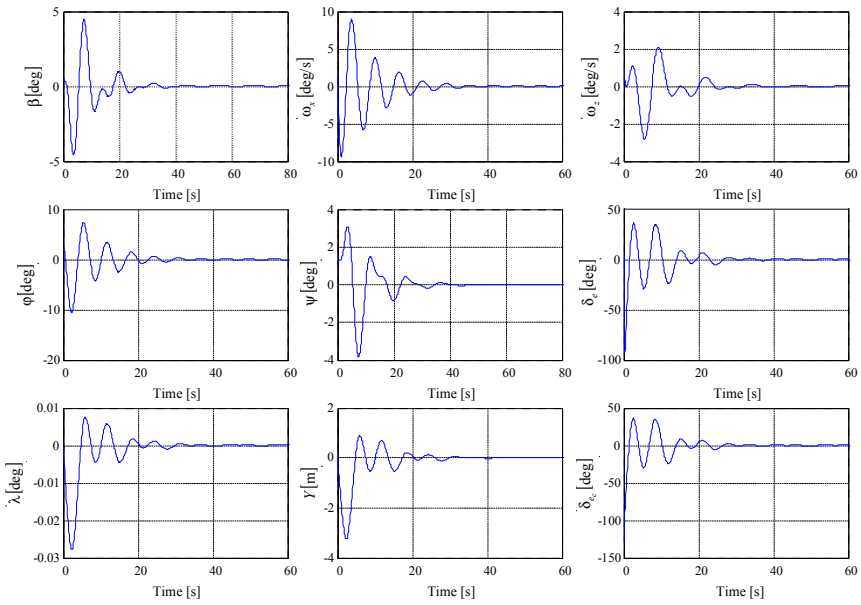

Fig. 7. Time characteristics associated to the initial approach phase

a strongly nonlinear dynamics. The H-inf technique's advantage is its applicability to situations implying multivariate systems with cross-coupling between the channels [20].

V. Conclusion

This work's purpose was the design of a complete ALS (longitudinal and lateral planes) using the H-inf technique; three landing subsystems have been designed: the first two are used to control the landing process in longitudinal plane (glide slope & flare), while the third one is the lateral plane (initial approach) intended. The three subsystems have been designed separately but these work together forming a single automatic landing system. The complete ALS has been software implemented, tested, and validated through numerical simulations; promising results have been obtained.

Acknowledgment

This work is supported by grant no. 89/1.10.2015 of the Romanian National Authority for Scientific Research and Innovation, CNCS-UEFISCDI, code PN-II-RU-TE-2014-4-0849.

References

[1] R. Lungu and M. Lungu, "Airplane Landing Control Using the H-inf Control and the Dynamic Inversion Technique," Chapter in the book „Automation and Control Trends", Intech Publisher, pp. 101-120, 2016.

[2] M. Lungu, "Flight control systems (Sisteme de conducere a zborului)," Sitech Publisher, Craiova, 2008.

[3] D. McLean, "Automatic Flight Control Systems," Prentice Hall Publisher, 1990.

[4] L. Zhi and W. Yong, "Intelligent landing of unmanned aerial vehicle using hierarchical fuzzy control", IEEE Aerospace Conference, 2012, pp. 1-12.

[5] Y. Ochi and K. Kanai, "Automatic approach and landing for propulsion controlled airplane by H-inf control," IEEE International Conference on Control Applications, Hawaii, pp. 997-1002, 1999.

[6] K. Nho and R. Agarwal, "ALS design using fuzzy logic," Journal of Guidance, Control and Dynamics, vol. 23, pp. 298-304, 2000.

[7] J. Juang and J. Chio, "Fuzzy modelling control for airplane automatic landing system," Int. Journal of Systems Science, vol. 36, no. 2, pp. 77-87, 2005.

[8] A. Calise, E.N. Johnson, M.D. Johnson, and J.E. Corban, "Applications of Adaptive Neural – Networks Control to Unmanned Aerial Vehicles," Journal of Harbin Institute of Technology, vol. 38, no. 11, 2006, pp. 1865-1869.

[9] A. Calise, S. Lee, and M. Sharma, "Direct Adaptive Reconfigurable Control of a Tailless Fighter Airplane", Rev. American Institute of Aeronautics and Astronautics, Georgia, USA, 2000.

[10] T. Wagner and J. Valasek, "Digital Autoland Control Laws Using Quantitative Feedback Theory and Direct Digital Design", Journal of Guidance, Control, and Dynamics, vol. 30, no. 5, pp. 1399-1413, 2007.

[11] J.O. Jang and G.J. Jeon, "A parallel neuro-controller for DC motors containing nonlinear friction," Neurocomputing, vol. 30, pp. 233-248, 2000.

[12] S. Seshagiri and H.K. Khalil, "Output feedback control of nonlinear systems using RBF neural network," IEEE Transactions on Neural Networks, vol. 11, pp. 69-79, 2000.

[13] B. Parkinson, M. O'Connor, and K. Fitzgibbon, "Airplane automatic approach and landing using GPS," Global Positioning System: Theory and Applications, vol. II, pp. 397-425, 1996.

[14] M. Lungu and R. Lungu, "Application of H_2/H_∞ Technique to Airplane Landing Control," Asian Journal of Control, vol. 17, no. 6, pp. 2153-2164, 2015.

[15] R. Lungu and M. Lungu, "Application of H_2/H_∞ and Dynamic Inversion Techniques to Airplane Landing Control," Aerospace Science and Technology, vol. 46, no. 1, pp. 146-158, 2015.

[16] J. Juang, H. Chang, and W. Chang, "Intelligent automatic landing system using time delay neural network controller," Applied Artificial Intelligence: An International Journal, vol. 17, no. 7, pp. 563-581, 2003.

[17] R. Lungu and M. lungu, "Airplane automatic control during landing (Controlul automat al aeronavelor la aterizare). Sitech Publisher, 2015.

[18] O. Yashimaso and K. Kimio, "Automatic Approach and Landing for Propulsion Controlled Airplane by H-inf Control," Proceedings of the IEEE International Conference on Control Applications, Hawaii, pp. 997-1002, 1999.

[19] R. Lungu, M., Lungu, and T.L. Grigorie, "ALSs with conventional and fuzzy controllers considering wind shears and gyro errors," Journal of Aerospace Engineering, vol. 26, no. 4, pp. 794-813, 2012.

[20] M. Lungu, R. Lungu, and D. Tutunea, "Control of Airplane Landing using the Dynamic Inversion and the H-inf Control," 17th International Carpathian Control Conference (ICCC 2016), Tatranská Lomnica, Slovak Republic, May 29 - June 1, pp. 461-466, 2016.

[21] R. Lungu, M., Lungu, and T.L. Grigorie, "Automatic control of airplane in longitudinal plane during landing," IEEE Transactions on Aerospace & Electronic Systems, vol. 49, no. 2, pp. 1338-1350, 2013.